Application of Amphiphilic 2-Acylamido-2-Methylpropane Sulfonic Acid - co-N-Isopropyl Acrylamide Nanogels as Thin Film Coatings

Ayman M. Atta[1,2,], Gamal A. El-Mahdy[1,3], and Hamad A. Al-Lohedan*

[1] Surfactants research chair, Department of Chemistry, College of Science, King Saud University, Riyadh 11451, Kingdom of Saudi Arabia.
[2] Egyptian Petroleum Research Institute, 1 Ahmad Elzomor St., Nasr city,Cairo, Egypt.
[3] Chemistry Department, Faculty of Science, Helwan University, Helwan, Egypt.
[*]E-mail: aatta@ksu.edu.sa

High surface active amphiphilic nanogels based on N-isopropyl Acrylamide-co- 2-acylamido-2-methylpropane sulfonic Acid (NIPAm/AMPS) prepared via free aqueous polymerization at room temperature have been prepared to apply as thin film anticorrosive coatings. The morphology and the particle size distribution of the nanogels were characterized transmission and scanning electron microscopy (TEM and SEM) and dynamic light scattering DLS in aqueous solution. The effectiveness of the synthesized compounds as corrosion inhibitors for carbon steel in 1 M HCl was investigated by various electrochemical techniques such as potentiodynamic polarization and electrochemical impedance spectroscopy (EIS). Results obtained from both potentiodynamic polarisation and EIS measurements reveal that the NIPAm/AMPS nanogel is an effective inhibitor for the corrosion of steel in 1.0 M HCl solution. Polarization data show that NIPAm/AMPS nanogel behaves as a mixed type inhibitor. The inhibition efficiencies obtained from potentiodynamic polarization and EIS methods are in good agreement.The results showed enhancement in inhibition efficiencies with increasing the inhibitor concentrations.

1. INTRODUCTION

There is a growing interest in the development of new families of amphiphilic nanogels because nanogel amphiphiles show a fascinating class of materials with unique properties, such as biomimics, ability for self-assembly, surface activity, ability to adsorb at interfaces, nano-encapsulation, and molecular recognition for medical and pharmaceutical applications [1-3]. The

preferred core-hydrophobic shell architecture, usually exhibit ordered aggregation on a nanoscopic scale with peculiar shapes and morphology. The amphiphilic nanogels can adapt to surrounding environments and change wettability and adhesion of different species on external stimuli [4, 5]. These materials are playing an increasingly important part in a diverse range of applications, such as biosensors, micro-electromechanical systems, and coatings that are capable of interacting with and responding to their environment [6-8]. Emerging applications extend to nanogel materials with rapidly adhesion to substrate to change wetting (from wettable to non-wettable), and coatings capable of rapid release of chemicals, as well as self-healing coatings [4, 5]. These advanced systems can be introduced into anticorrosive coatings at a relatively low cost, because often only a very thin (nanometer thick) coating is required.

The preparation of polymeric nanoparticles attracted more attention due to their size, surface features and functionalities can be controlled [9]. The Polymeric nanoparticle can be prepared using two major approaches: (1) fabrication of the particles from pre-synthesized polymers and (2) synthesis of reactive nanoparticles by a heterogeneous polymerization method [10].One of the most important method used to prepare microgels[11], crosslinked nanoparticles, their composites [12], is crosslinking polymerization. The crosslinked systems have many commercial applications in the paints, and powder coatings. The Cross-linked nanoparticles are formed in homogeneous solutions or in emulsion medium. Emulsion polymerization [13, 13], radiation polymerization [15], dispersion polymerization [16], distillation-precipitation polymerization [17] and self-assembly method [18] are often used to prepared polymer particles. Polymer based nanoparticles can be also prepared by the well-known solvent evaporation method in which the droplets of a nanoemulsion are composed of a volatile organic solvent in which the polymer is solubilized [19]. In the previous work [20], poly (vinylpyrrolidone) (PVP) is an initial core of poly (2-acrylamido-2-methylpropane sulfonic acid) (PAMPS) nanogels, and the core was formed in water/ acetone cosolvent. An innovative synthesis method was used to synthesize PAMPS/PVP nanogels directly in an aqueous system. In particular, much attention is being given to temperature-responsive nanogels consisting of a lightly crosslinked polymer chain of *N*-isopropylacrylamide (NIPAm). In this respect, nanogel particles based on amphiphilic crosslinked NIPAm and 2-acrylamido-2- ethylpropane sulfonic acid (AMPS) copolymer nanogel (NIPAm/AMPS)showed high surface activity and high adsorption affinity at interface [21]. In this article, it was expected that the application of nanogel particles to protect the steel from corrosion inhibition protection can forms a uniform thin film on the surface of steel which provide advantages over normal organic inhibitors. The objective of this paper is to apply NIPAm/AMPS nanogel as corrosion inhibitors for carbon steel in 1 M HCl solution. The inhibition efficiency was menitored by electrochemical techniques (potentiodynamic polarization curves and electrochemical impedance spectroscopy).

2. EXPERIMENTAL

2.1. Materials

2-Acrylamido-2-methylpropane sulfonic acid (AMPS), *N*-isopropylacrylamide (NIPAm), N,N-methylenebis-acrylamide (MBA), ammonium persulfate (APS) and tetramethylenethylendiamine

(TEMED) were delivered from Aldrich chemicals Co. Corrosion tests were performed on carbon steel electrode having the following chemical composition (wt.%): 0.3% C, 0.02% Si, 0.03% Mn, 0.045% Sn, 0.04% P and the remainder Fe. The experiments were performed with steel specimens with the following chemical composition (wt.%): 0.14% C, 0.57% Mn, 0.21% P, 0.15% S, 0.37% Si, 0.06% V, 0.03% Ni, 0.03% Cr and the remainder Fe. Prior to experiments, the specimens were successively polished using emery papers from 100 to 4000 grade. Then, the specimens were washed with distilled water and degreased with acetone and dried with a cold air.

2.2. Polymerization technique of NIPAm/AMPS:

Crosslinked NIPAAm/AMPS, was prepared through a modified temperature programmed in the presence of water as a solvent and free surfactant technique as described in our previous work [21]. NIPAm (90 mol %) was used to copolymerize with AMPS (10 mol %) monomer. In this respect, the NIPAm monomer (10 mol % from 90 mol%) was agitated in 40 ml of water and preheated to 40 ^{o}C for 30 minute under nitrogen atmosphere. A catalytic amount of a TEMED solution (0.32 M) dissolved in 5 ml water injected to initiate the polymerization. The reaction temperature was increased up to 55 ^{o}C with rate 5 ^{o}C per 15 minute. The NIPAm, AMPS, and MBA were dissolved in 20 ml of water and mixed with APS dissolved in 45 ml of water and then injected with rate 1 ml/minute by means of a syringe pump under stirring. The reaction temperature kept at 60 ^{o}C for 2 hrs. The resultant nanogels were seperated by ultracentrfugation at 25000 rpm and the resultant particles were dispersed in water and repreciptated in 10 fold of acetone.

2.3. Characterization of the prepared NIPAm/AMPS nanogel

Transmission electron microscopy (TEM) micrographs were taken with a JEOL JEM-2100F (JEOL, Tokyo, Japan). A few drops of magnetite nanoparticle solution were diluted into 1 mL of ethanol, and the resulting ethanol solution was placed onto a carbon coated copper grid and allowed to evaporate. HR-TEM images of the nanocomposites were recorded using a JEM-2100F (JEOL) at an acceleration voltage of 200 kV.

SEM images were taken with Gemini microscope DMS-982 (Zeiss, Germany). Diluted dispersions of nanoogel in distilled water (100μg/ml) were prepared, sonicated for 5min at room temperature and filtered through a 0.45μm cellulose acetate filter. The filtrate was placed on the aluminium foil followed by air drying. The dried films were placed on the SEM sample stage and coated with gold to increase the contrast and quality of the images.

Samples for dynamic light scattering (DLS) were prepared by dispersion several drops of the diluted nanoparticle solution into 2 mL of water under vigorous stirring. The DLS measurements were performed on a Brookhaven Instruments system (Santa Barbara, CA, USA) with a 514.5 nm argon ion laser (model 85 Lexel Laser) as the light source.

2.4. Electrochemical measurements

A three-electrode system including a steel as working electrode (WE) , Pt sheet as counter electrode (CE) and saturated calomel electrode (SCE) as a reference electrode (RE) were used for electrochemical measurement. Potentiodynamics polarization measurements were conducted with a computer-controlled (potentiostat/galvanostat) Solartron 1470E system. Polarization curves were carried out by using a scna rate of 1mV/sec. Impedance measurements were carried out using Solartron 1470E system (potentiostat/galvanostat) with Solartron 1455A as frequency response analyzer in the frequency range of 10 mHz–100 kHz using a 10 mV peak-to-peak voltage excitation. Data were collected and analysed using CorrView, Corr- Ware, Zplot and ZView software.

3. RESULTS AND DISCUSSION

In the previous work [21], several types of NIPAm/AMPS nanogels were prepared using aqueous radical polymerization technique. We selected NIPAm/AMPS (90/10 mol %) to apply as anticorrosive thin film for steel. The TEM and SEM analyses were used to study the morphologies of the prepared nanogels. The particle size distribution was measured by DLS measurements. In this respect, TEM micrograph was represented in Figure 1.
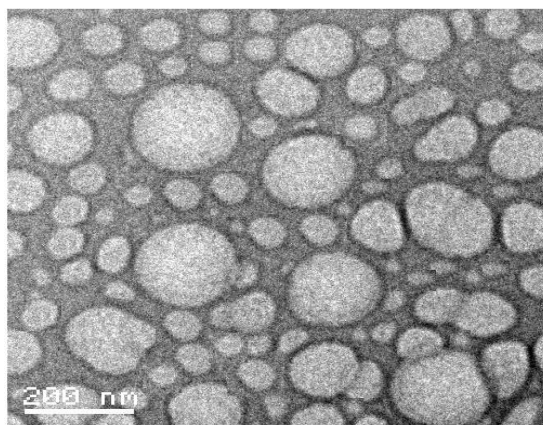

Figure 1. TEM micrograph of NIPAm/AMPS (90/10 mol%) nanogel.

TEM analysis indicated that the formation of eclipsed spherical particle of NIPAm/AMPS nanogel. It is appeared non-uniform dark periphery which indicated the higher crosslinked density and complex interlaced structure of NIPAm/AMPS networks. TEM analysis indicated that the average particle diameters ranged from 55 up to 165 nm. Moreover, it is noticed that NIPAm/AMPS nanogels dried powder is easy to redisperse in distilled water to nanogel solutions. The mean diameter of the nanogels after redispersion shows insignificant change.

Figure 2 illustrates the SEM image of NIPAm/AMPS (90 mol % / 10 mol %). It was observed that the particles showed spongy spherical morphology with aggregates which comparable to TEM

graphs (Figure 1). The SEM micrograph indicates that the formation of microparticles during synthesis of NIPAm/AMPS nanoparticles. The SEM image shows that the particles are well-dispersed spherical particles.
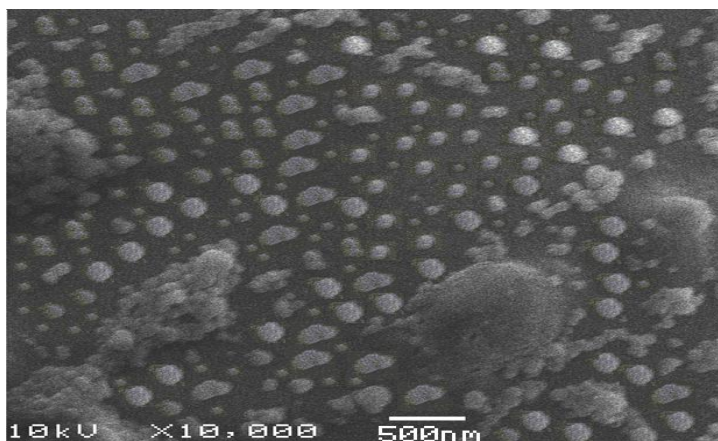

Figure 2. SEM micrograph of NIPAm/AMPS (90/10 mol%) nanogel.

The accurate particle size distribution canbe determined from DLS measurements. The DLS data was illustrated in Figure 3. The data revealed that the NIPAm/AMPS (90/10 mol%) nanogel is polydisperse in aqueous media with particle size ranged from 30 to 300nm. The data of Fig. 3 indicate that the average particle sizes obtained using this technique are much larger than those obtained using TEM. This was referred to the hydrophilicity of nanogels NIPAm/AMPS increased the particle size due to swelling [22-24]. Moreover, the low particle size of TEM imaging, possibly because they are disturbed due to the drying forces present during TEM sample preparation [25].
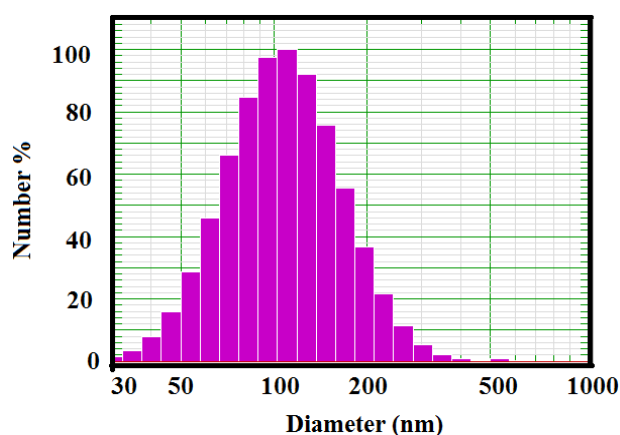

Figure 3. DLS measurement of dispersed NIPAm/AMPS (90/10 mol%) nanogel diluted aqueous solution.

3.2. Potentiodynamic polarization

Potentiodynamic polarization curves for corrosion of steel in 1M HCl, solutions without and with NIPAm/AMPS nanogels were   shown in Figure 4. The presence of NIPAm/AMPS nanogels causes a prominent shift for both anodic and cathodic curves to lower values of current densities. The anodic and cathodic   reactions of steel   are   clearly inhibited with increasing the concentration of nanogels.
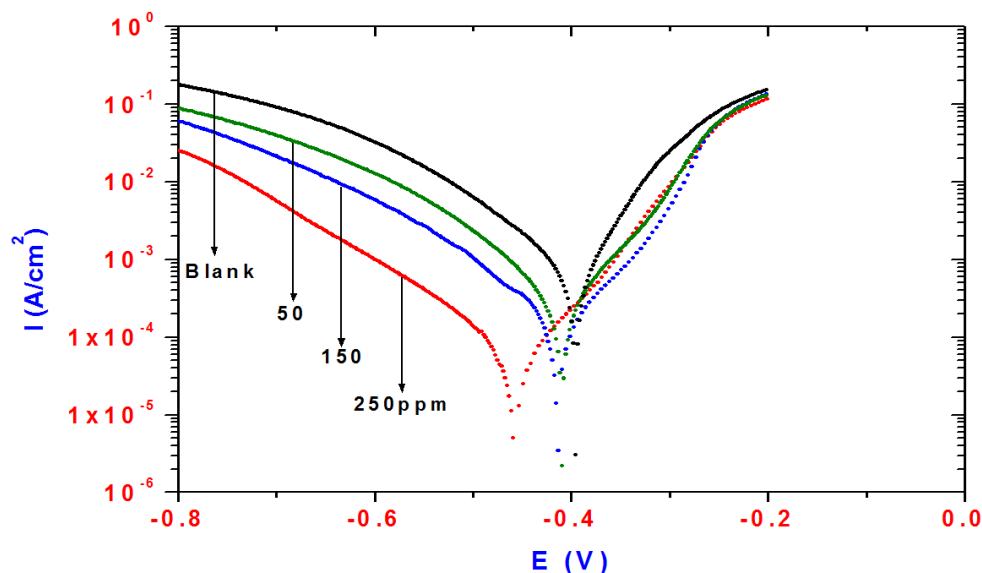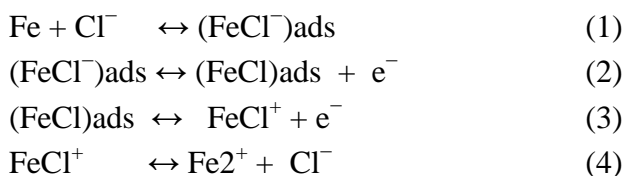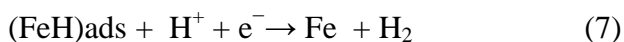

Figure 4. Polarization curves for steel in 1M HCl solution containing different concentrations of NIPAm/AMPS nanogels .

This result suggests that addition of NIPAm/AMPS nanogels in 1M HCl, solutions reduces significantly anodic dissolution and retards the cathodic reaction of steel.   These phenomena clearly indicate that NIPAm/AMPS nanogels acts essentially as a mixed type inhibitor in 1M HCl, solutions. The inhibition action is caused by geometric blocking effect by a reduction of the active sites area on the surface of the corroding steel [26]. It can be concluded that both cathodic and anodic reactions of steel corrosion are drastically retarded by the addition of NIPAm/AMPS nanogels in   1M HCl, solutions. The anodic dissolution of iron may be described as follows: [27]:

$$Fe + Cl^- \leftrightarrow (FeCl^-)ads \qquad\qquad (1)$$
$$(FeCl^-)ads \leftrightarrow (FeCl)ads + e^- \qquad\qquad (2)$$
$$(FeCl)ads \leftrightarrow FeCl^+ + e^- \qquad\qquad (3)$$
$$FeCl^+ \leftrightarrow Fe2^+ + Cl^- \qquad\qquad (4)$$

The cathodic hydrogen evolution reaction may be given as follow:

$$Fe + H^+ \leftrightarrow (FeH^+)ads \qquad\qquad (5)$$

$$(FeH^+)ads \ + \ e^- \rightarrow (FeH)ads \qquad\qquad (6)$$

$$(FeH)ads + \ H^+ + e^- \rightarrow Fe \ + H_2 \qquad\qquad (7)$$

It is suggested that the oxidation reaction shown by equations (1) to (4) can be inhibited [28-31] by blocking effect of reaction area on the corroding surface. The adsorbed NIPAm/AMPS nanogels also block the active sites of hydrogen evolution on the Fe surface and inhibits the reactions presented in equations from 5 to 7. It is expected that, a higher coverage of the inhibitor film on the steel surface forms at higher inhibitor concentrations.

Accordingly, the corrosion current density values are estimated accurately by extrapolating the cathodic and anodic linear region to the corrosion potential.

Table 1. Inhibition efficiency values for steel in 1M HCl with different concentrations of NIPAm/AMPS nanogels calculated by Polarization and EIS methods.

Polarization Method						EIS Method		
	Ba (mV)	Bc (mV)	E_{corr} (V)	i_{corr} $\mu A/cm^2$	$IE\%$	R_{ct} Ohm	Cdl ($\mu F/cm^2$)	$IE\%$
Blank	69	120	-0.3955	839	_____	1.80	334	____
50 ppm	73	78	-0.4092	257	69	7.61	157	76.00
150	74	101	-0.4128	133	84	13.80	120	87.00
250	79	108	-0.4573	54	94	20.00	113	91.00

The electrochemical corrosion parameters including corrosion current densities (i_{corr}), corrosion potential (E_{corr}), anododic Tafel slope (Ba), cathodic Tafel slope (Bc) and corresponding inhibition efficiency ($IE\%$) are given in Table 1. The inhibition efficiency (IE%) was calculated from potentiodynamic polarization using the following relationship [32-34]:

$$IE\% = 1 - i_{corr\,(inh)} / i_{corr\,(uninh)} \text{ x } 100 \qquad\qquad (1)$$

where $i_{corr(uninh)}$ and $i_{cor(inh)}$ are corrosion current density values in the absence and presence of inhibitor, respectively. The inhibition efficiencies (*IE%*) were also listed in Table 1. As can be seen from Table 1, corrosion current decreases drastically in the presence of inhibitor and decreases with increasing the inhibitor concentration. It is evident that IE% increases with the inhibitor concentration, due to an increase in the blocked area of active sites of the steel surface. The decrease of corrosion rate may be explained by the inhibitory action of inhibitor on cathodic and anodic branches of the polarization curves by blocking the anodic and cathodic active sites on steel surface. Accordingly, NIPAm/AMPS nanogels behaves as a mixed type inhibitor [35–38].

3.3. Electrochemical impedance spectroscopy (EIS)

Figure 5 shows the typical Nyquist diagram for corrosion of steel in 1 M HCl solution with and without NIPAm/AMPS nanogels. The impedance diagrams consist of single semicircle capacitive loop indicating a charge-transfer process mainly controlling the corrosion of steel. The EIS plots can be interpreted by an equivalent circuit composed of a solution resistance (Rs), a charge transfer resistance (Rct) and a double layer capacitance (Cdl). The circuit employed allows the identification of both charge transfer resistance (Rct) and double layer capacitance (Cdl). The fit parameters were analyzed using Zview2 software and listed in Table 1.
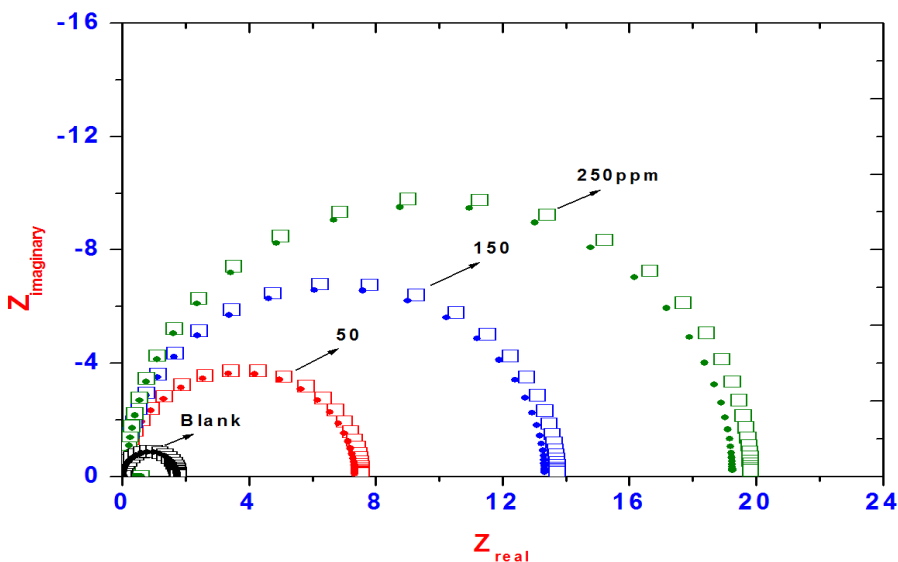

Figure 5. Nyquist plot for steel for steel in 1m HCl solution containing different concentrations of NIPAm/AMPS nanogels.

The inhibition efficiencies (*IE%*) for the corrosion of steel were calculated and also listed in Table 1 by means of the following equation [39-41]:

$$IE\% = 1 - R^{o}ct / Rct_{(inh)} \tag{2}$$

where $R^{o}ct$ and $Rct_{(inh)}$ are the values of the charge transfer resistance

without and with inhibitor, respectively. As can be seen from the data presented in Table 1, the inhibition efficiencies increase significantly with the concentration of inhibitor. It can be concluded that , NIPAm/AMPS nanogels exhibits effective inhibition for the corrosion of steel in 1 M HCl solution. As the inhibitor concentration increased, the Rct values increased, but the Cdl values tended to decrease. The decrease in Cdl value may be accounted to the adsorption of inhibitor on steel surface, which led to an increase in IE%. In addition, the decrease in the Cdl values can be attributed to a decrease in local dielectric constant and/or an increase in the thickness of the electrical double layer, which enhance the adsorption of inhibitor on the steel surface. The inhibition efficiencies, calculated from potentiodynamic polarization curve and EIS measurements are in reasonably good agreement

4. CONCLUSIONS

1.   NIPAm/AMPS nanogels   was an effective inhibitor for corrosion of steel in 1M HCl solution and the inhibition efficiency increased with increasing concentration.

2.   NIPAm/AMPS nanogels inhibits the corrosion of steel by controlling both anodic and cathodic reactions in 1M HCl solution and acts as a mixed type inhibitor.

3. Results from potentiodynamic polarization curve and EIS measurements are in a reasonably good agreements and points to the fact that NIPAm/AMPS nanogel is a good corrosion inhibitor for steel in acidic chloride solution.

References

1. 1. S.akeda, H.Takahashi, S, Sawada, Y. Sasaki, K. Akiyoshi, *RSC Adv.*, 3 (2013) 25716.
2. Y. Nomuraa, Masahiro Ikedaa, Nozomi Yamaguchib,Yasuhiro Aoyamaa, Kazunari Akiyoshic,FEBS letters, Volume 553, Issue 3, 23 October 2003, Pages 271–276.
3. A. M. Atta, O. E. El-Azabawy, H.S. Ismail, M.A. Hegazy, Corrosion Science 53 (2011) 1680.
4. M. Plawecka, D. Snihirova, B. Martins, K.Szczepanowicz, P. Warszynski, M.F. Montemor, *Electrochimica Acta,* 140 (2014)282.
5. Anna C. Balazs,*Materials Today, 10 (2007)*18.
6. P. M. Mendes, *Chem. Soc. Rev.,* 37 (2008)2512.
7. I. Luzinov, S. Minko, V. V. Tsukruk, *Soft Matter,*4 (2008)714.
8. M. Motornov, *Langmuir,* 19 (2003) 8077.
9. J.L. Turner, K.L. Wooley, *Nano Lett*., 4(2004)683.
10. 10- M. Motornov, Y. Roiter, I. Tokarev, S. Minko, *Progress in Polymer Science,* 35 (2010) 174.
11. L. Valette, J.P. Pascault, B. Magny *Macromol. Mat. Eng.,* 288, (2003)642.
12. Y. Wang, X.W. Teng, J.S. Wang, H. Yang, *Nano Lett.,* 3 (2003)789.
13. H. Tobia, M. Kumagai, N. Aoyagi, *Polymer,* 41(2000)481.
14. S.V. Vinogradov, T.K. Bronich, A.V. Kabanov, *Adv. Drug Deliver Rev.,*54 (2002)135.
15. J.M. Rosiak, I. Janik, S. Kadlubowski, *Nucl. Instrum Meth* B 208: (2003) 325–330
16. I. Capek, *Adv. Colloid Interface Sci.,* 88 (2000) 295.
17. F. Bai, X.L. Yang, W.Q. Huang, *J. Appl. Polym. Sci*., 100 (2006) 1776.
18. B.L. Guo, J.F. Yuan, L. Yao, *Colloid Polym. Sci.,* 285(2007)665.
19. S. Vemuri, C.T. Rhodes, *Pharm. Acta Helv*. 70 (1995) 95.
20. A. M. Atta, R. A. M. El-Ghazawy, R.K. Farag, S.M. Elsaeed, *Polym. Adv. Technol.*, 22 (2011)732.
21. *A. M. Atta, H . Al-Shafey, Int. J. Electrochem. Sci.,* 8 (2013) 4970.
22. A. V. Kabanov, S. V. Vinogradov, *Angew Chem Int Ed Engl.,* 48 (2009)5418.
23. G. Deepa, A. Kumar, T. Thulasidasan, R. J. Anto, J. J. Pillai, G.S.V. Kumar, *International Journal of Nanomedicine,* 7 (2012)4077.
24. 24. G. Aguirre, J. Ramos, J. Forcada, *Soft Matter*, 9 (2013) 261.
25. M. A. Akl, A. M. Atta, A. E-F.M. Yousef, M. I. Alaa, *Polym. Int.,* 62 (2013) 1667.
26. C. Cao, *Corros. Sci*. 38 (1996) 2073.
27. R. Solmaz, G. Kardas,   , B. Yazıcı, M. Erbil, , *Colloid Surf. A* 312 (2008) 7.
28. Q.B. Zhang, Y.X. Hua, , *Electrochim. Acta* 54 (2009) 1881.
29. A. Yurt, A. Balaban, S. Ustun Kandemir, G. Bereket, B. Erk, , *Mater. Chem. Phys*. 85 (2004) 420.

30. H. Keles, , M. Keles, , I. Dehri, O. Serinda˘g, *Mater. Chem. Phys*. 112 (2008) 173.
31. R. Solmaz, G. Kardas, , M. C, ulha, B. Yazıcı, M. Erbil, *Electrochim. Acta* 53 (2008) 5941.
32. Q. Qu, Z. Hao, L. Li, W. Bai, Z. Ding, *Corros. Sci*. 51 (2009) 569.
33. F. Bentiss, M. Lebrini, M. Lagrenée, *Corros. Sci*. 47 (2005) 2915.
34. Q. Qu, S. Jiang, W. Bai, L. Li, *Electrochim. Acta* 52 (2007) 6811.
35. M. Finsgar, *Corros. Sci*. 72 (2013) 82.
36. A. El Bribri, M. Tabyaoui, B. Tabyaoui, H. El Attari, F. Bentiss, *Mater. Chem. Phys*. 141 (2013) 240.
37. M.A. Abu-Dalo, N.A.F. Al-Rawashdeh, A. Ababneh, *Desalination* 313 (2013) 105.
38. F. Bentiss, M. Lebrini, M. Lagrenée, *Corros. Sci*. 47 (2005) 2915.
39. S. Rames, S. Rajeswari, *Electrochim. Acta* 49 (2004) 811.
40. E. Chaieb, A. Bouyanzer, B. Hammouti, M. Benkaddour, *Appl. Surf. Sci.* 246 (2005) 199.
41. A. Dadgarnezhad, I. Sheikhshoaie, F. Baghaei, *Anti-Corros. Meth. Mater*. 51 (2004) 266.